

Analysis and Design of an Inverted-F Antenna Printed on a PCMCIA Card for the 2.4 GHz ISM Band

C. Soras, M. Karaboikis, G. Tsachtsiris, and V. Makios

Laboratory of Electromagnetics, Department of Electrical and Computer Engineering, University of Patras
26500 Rio-Patras, Greece
Tel: +30 (61) 997 344, Fax: +30 (61) 997 342,
E-mail: soras@ee.upatras.gr, manosk@loe.ee.upatras.gr, tsachtsiris@loe.ee.upatras.gr, v.makios@ee.upatras.gr

Abstract

The development of small integrated antennas plays a significant role in the progress of rapidly expanding commercial communication applications. This paper addresses the analysis and design of an inverted-F antenna (IFA) printed on a PCMCIA card. The antenna is compact, easy to manufacture, and efficient, with an omni-directional pattern and a bandwidth of 250 MHz. The performance of the integrated IFA/PCMCIA system was simulated using two commercial Method of Moments codes, and validated with measurements on a fabricated prototype.

Keywords: Microstrip antennas; inverted F; omni directional antennas; ISM band; wireless LAN; mobile antennas

1. Introduction

The use of the 2.4 GHz industrial, scientific, and medical (ISM) band is becoming an important means of wireless communication. Wireless local-area networks (WLAN), wireless Internet at any access-point-equipped building, and the planned development of Bluetooth all utilize the 2.4 GHz ISM band. Furthermore, an enormous number of potential applications based on these technologies are possible in the future. Therefore, the development of appropriate antenna designs is imperative.

A group of candidate antenna structures that might be considered for use in short-range radio devices is made up of the printed dipole, the microstrip patch, the ceramic antenna, and the monopole and its variants. The printed dipole has a favorable radiation pattern, but its relatively large size and the need for a differential feed make it unsuitable for many devices. The microstrip-patch antenna has no production cost and we can choose a desired polarization, but it has small bandwidth. The ceramic antenna does not have negligible cost per unit, and its efficiency is medium. The monopole is a variant of the dipole that uses the device's ground plane to provide the other half of the antenna. The inverted-L and the inverted-F antennas fall into this category. The inverted-F antenna is well known for its ability to provide flexibility in impedance matching, and to produce both vertically and horizontally polarized electric fields [1], a feature that is desirable for indoor environments.

The objective of this paper is primarily to present an inverted-F antenna (IFA) for the 2.4 GHz ISM band that is printed on a PCMCIA (Personal Computer Memory Card International

Association) card. It incorporates desirable characteristics, such as no additional cost, ease of manufacture, compact size, acceptable bandwidth, high efficiency, and a good omnidirectional radiation pattern. Furthermore, a detailed study of the geometric parameters that influence the tuning of the antenna was carried out, in order to help the antenna designer to modify its dimensions according to the available space on the card, or any other restrictions he or she might have. It should be clarified that the antenna presented is a printed IFA, and not a planar IFA (PIFA). To the best of our knowledge, this is the first detailed work on this configuration.

The second section of the paper is devoted to the theoretical and geometric characteristics of the printed IFA/PCMCIA system, with an emphasis on the ground-plane effect. In the third section, the simulation results based on the Method of Moments are illustrated, along with measurements made on a fabricated prototype. Finally, the influence of the IFA's geometric parameters on its operation and related design guidelines are discussed in the fourth section.

2. The Integrated Printed IFA/PCMCIA Card System

The geometry and dimensions of the implemented printed inverted-F antenna are depicted in Figure 1. The inverted-F antenna is a variant of the monopole, where the top section has been folded down so as to be parallel with the ground plane. This is done to reduce the height of the antenna, while maintaining a resonant trace length. This parallel section introduces capacitance

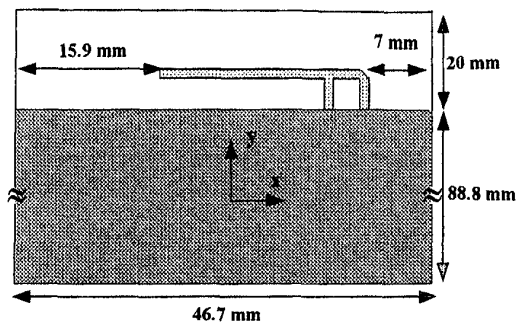


Figure 1a. A top view of the geometry of the IFA/PCMCIA card system.



Figure 1b. A cross section of the geometry of the IFA/PCMCIA card system.

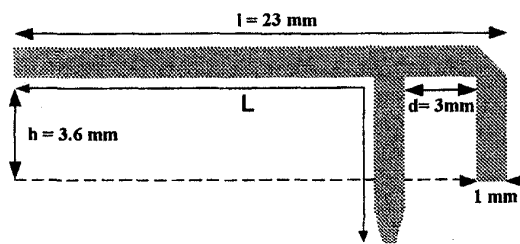


Figure 1c. The IFA's dimensions.

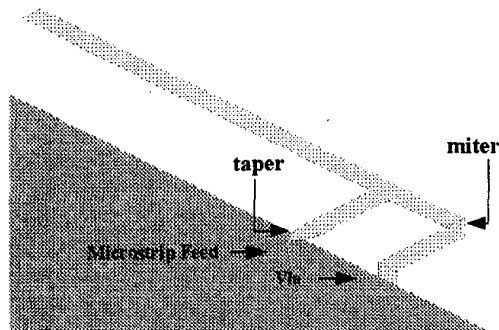


Figure 1c. The IFA's connection to the PCMCIA circuitry.

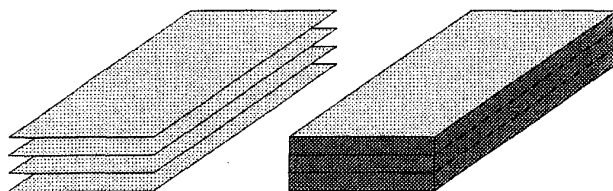


Figure 1e. The metallic layers unconnected, and connected with rectangular vias.

to the input impedance of the antenna, which is compensated for by implementing a short-circuit stub. The stub's end is connected to the ground plane through a via. The width of the antenna trace is $w = 1$ mm, and its physical length is $L = 28.1$ mm. A microstrip feed is used to connect the antenna to the PCMCIA card's circuitry. The printed IFA is placed close to the edge of the PCMCIA card, which consists of four metallic layers, with the antenna placed on the upper layer. The card has dimensions of 46.7 mm by 108.8 mm and a thickness of 0.8 mm (± 4 mils tolerance), with the second-from-the-top layer being the card's ground plane. The thickness of the copper layers is $t = 48.26 \mu\text{m}$, the copper's conductivity is $\sigma = 5.8 \times 10^7 \text{ S/m}$, and the relative dielectric constant is $\epsilon_r = 3.93$ with $\tan \delta = 0.01$.

The four metallic layers of the PCMCIA card are interconnected through conducting vias, forming a ground plane for the antenna, which plays a significant role in its operation. Excitation of currents in the printed IFA causes excitation of currents in the ground plane such that at a distance, the resulting electromagnetic field is formed by the interaction of the IFA and an image of itself below the ground plane. Its behavior as a perfect energy reflector is consistent only when the ground plane is infinite, or very much larger in its dimensions than the monopole itself. In our case, the PCMCIA's metallic layers are of comparable dimensions to the monopole, and act as the other part of the dipole. The antenna/PCMCIA combination will now behave as an asymmetric dipole, the differences in current distribution on the two-dipole arms being responsible for some distortion of the radiation pattern. In general, the required PCB ground-plane length is roughly one-quarter of the operating wavelength, λ . To the extent that the ground plane is much longer than $\lambda/4$, the radiation patterns will become increasingly multi-lobed. On the other hand, if the ground plane is significantly smaller than $\lambda/4$, then tuning becomes increasingly difficult, and the overall performance degrades [2]. The optimum location of the IFA – in order to achieve an omnidirectional far-field pattern and 50Ω impedance matching – was found to be close to the edge of the PCMCIA card, as illustrated in Figure 1a.

Some techniques, which were also used to optimize the operation of the IFA/PCMCIA system, concern the miter and taper shown in Figure 1d. The miter is used to avoid a right-angle microstrip bend, which results in a poor current flow on the stub. The optimum miter was calculated using the formula presented in [3]. As far as the taper is concerned, its need arose in order to compensate for the 8-to-40-mils abrupt-step transition encountered between the microstrip-line feed and the antenna. After several impedance-matching tests with different kinds of tapers [4], the optimum taper was found to be the curved taper.

3. Simulated and Measured Results

The geometry shown in Figure 1 was analyzed, using two Method-of-Moments-based electromagnetic-field solvers, *IE3D* [5] and *ADS Momentum* [6]. The validation of the simulated results was performed by computing the return loss at the antenna port, and comparing it with measurements on the fabricated prototype. In both *IE3D* and *ADS*, the highest meshing frequency was set at 4.5 GHz, with 20-cells-per-wavelength discretization and edge-meshing, to achieve high accuracy in the calculation of the current distribution. As proposed in [7], an edge cell of 10% of the strip width – that is, 0.1 mm – was used. From Figure 2, it can be

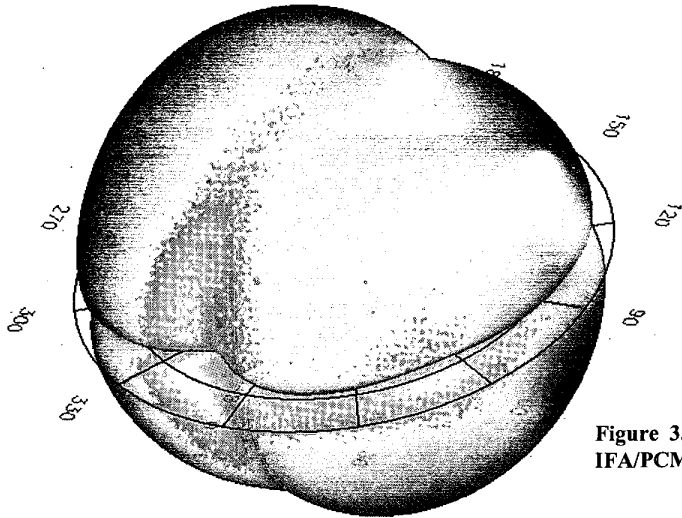


Figure 3. The three-dimensional gain pattern of the printed IFA/PCMCIA system.

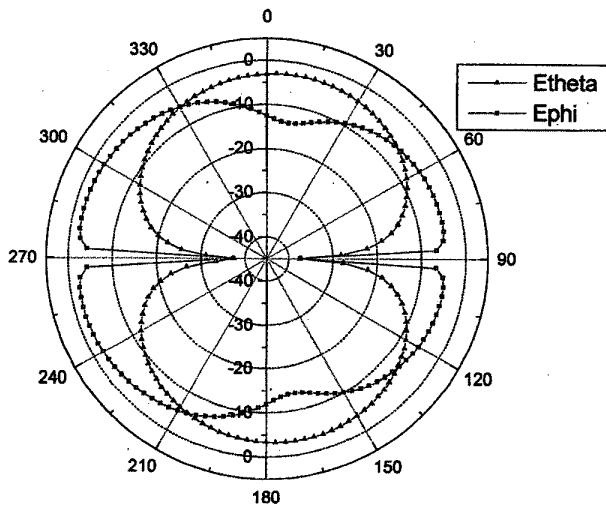


Figure 4a. The gain pattern of the printed IFA/PCMCIA system (dBi): x - z cut.

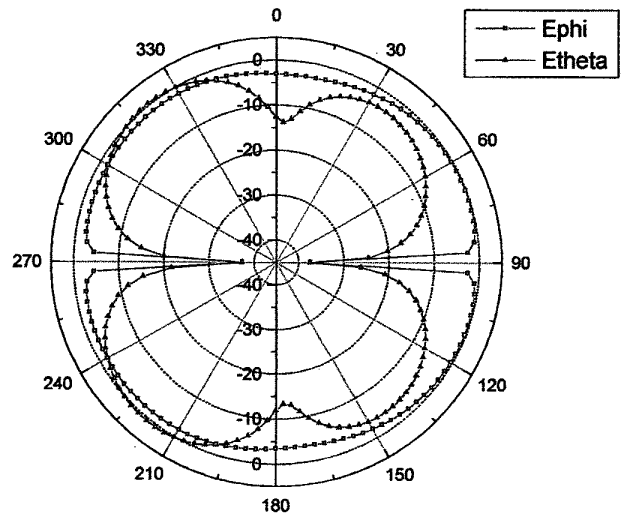


Figure 4b. The gain pattern of the printed IFA/PCMCIA system (dBi): y - z cut.

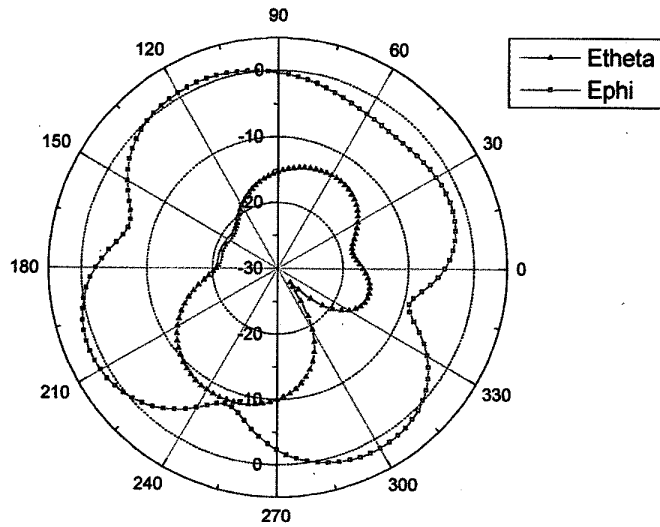


Figure 4c. The gain pattern of the printed IFA/PCMCIA system (dBi): x - y cut.

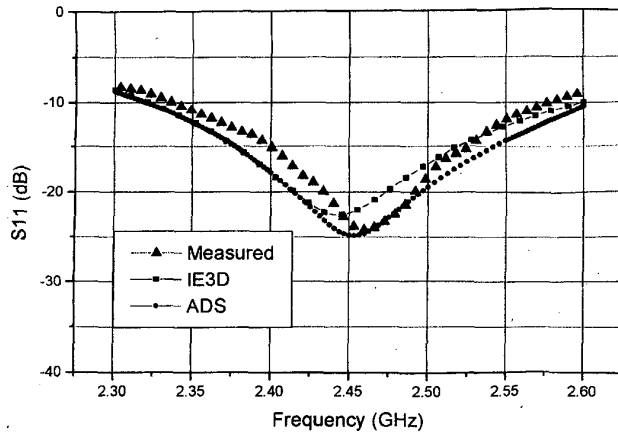


Figure 2. The return loss (S_{11}) of the printed IFA.

inferred that both *ADS* and *IE3D*'s predictions of the return-loss values (S_{11}) agree very well with the measured values, and that the printed IFA is well tuned for this ISM band

Figure 3 illustrates the three-dimensional gain pattern of the IFA/PCMCIA system, while in Figure 4 the components E_θ and E_ϕ at the three principal orthogonal planes are depicted. These figures show the omni-directional behavior of the antenna. The gain values insure adequate performance for typical indoor environments, taking into account the standard values of the output power and receiver sensitivity of short-range radio devices. It is also worth mentioning that the polarization of the antenna is rather more elliptical than linear, since the axial ratio rarely reaches 20 dB [8]. Thus, the antenna has the ability to receive both vertically and horizontally polarized electromagnetic waves. This can prove beneficial in indoor environments, where depolarization is a dominant phenomenon and the choice of the best polarization is difficult. Although, currently, many wireless systems are vertically polarized, it has been predicted [9] that using horizontal antennas at both the receiver and the transmitter will result in 10 dB more power, in the median, as compared to the power received using vertical antennas at both ends of the link.

To evaluate the performance of the printed IFA in an indoor environment, we performed some initial field tests, where we measured the packet-error rate (PER) of a Bluetooth application under two scenarios: a) using external vertically polarized monopole antennas at both ends, and b) using two printed IFAs. The measurements were taken inside a typical office environment, under both line-of-sight and non-line-of-sight conditions at a 1 Mb rate of transmission. Although the results showed a slight benefit of the external monopoles over the IFAs, the no additional cost and the low profile of the IFA overwhelm the small difference in the reception, which for all cases was less than 10%. Other radiation parameters of the antenna system as implemented are presented in Table 1.

An interesting insight to the complex relations between the IFA's feed and the PCMCIA's metal layers is gained by examining the currents flowing on the surfaces of the four layers. If there is no connection between the four layers, some of the power feeding the antenna is launched into the parallel-plate mode, shown in Figure 5a (a_1 , a_2 , a_3 , a_4 , from bottom to top). The result of this effect is the appearance of the four resonances shown in Figure 6,

two of which fall into the pass band of the antenna, distorting its impedance matching. By connecting the edges of the four layers through rectangular conducting vias, we simulate the existence of the via holes in the perimeter of the prototype card (Figure 1e). In this case, the power in the parallel-plate mode is drastically reduced, as shown in Figure 5b, resulting in the absence of the resonances observed in Figure 2. It should be pointed out that the location of the mode-suppressing vias was found to be critical, and that for a successful design, the effect of the vias must be included in the analysis.

4. Discussion

Three geometric parameters of the antenna play a critical role for its tuning: the height, h , the distance between the two legs, d , and the length, l [10, 11]. What makes the printed IFA a good candidate for this application – beyond the low profile and the high bandwidth – is the ability to match the input impedance of the antenna very easily. Figure 7 displays the input impedance of the printed IFA as a function of the lengths h , d , and l from 2.3 to 2.6 GHz. These lengths were normalized to the free-space wavelength at the middle frequency of the band ($\lambda_0 = 122.45$ mm), and each time, we varied one parameter while keeping the values of the other two fixed. According to Figure 7, the three controlling

Table 1. The radiation parameters of the IFA/PCMCIA card system.

Radiation Parameters	IE3D			ADS		
	2.4 GHz	2.45 GHz	2.4835 GHz	2.4 GHz	2.45 GHz	2.4835 GHz
Max at (θ, ϕ)	40.270	40.270	40.270	42.279	42.276	42.276
Directivity (dBi)	3.23	3.19	3.17	3.25	3.22	3.20
Gain (dBi)	2.52	2.50	2.49	2.64	2.63	2.62
Efficiency (%)	85.96	85.97	86.22	86.72	86.88	86.98

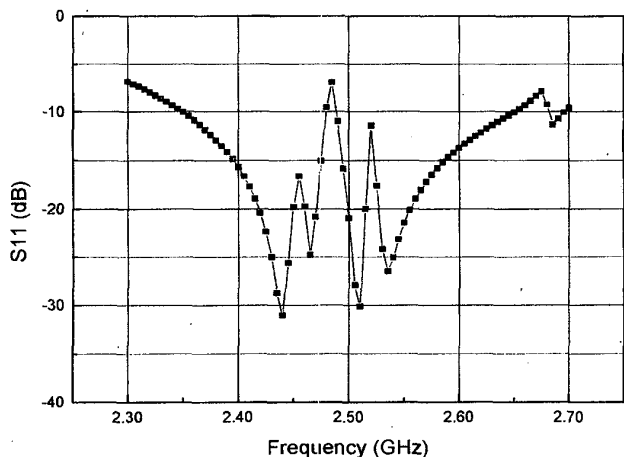


Figure 6. The return loss (S_{11}) of the printed IFA if the metallic layers of the PCMCIA card were unconnected.

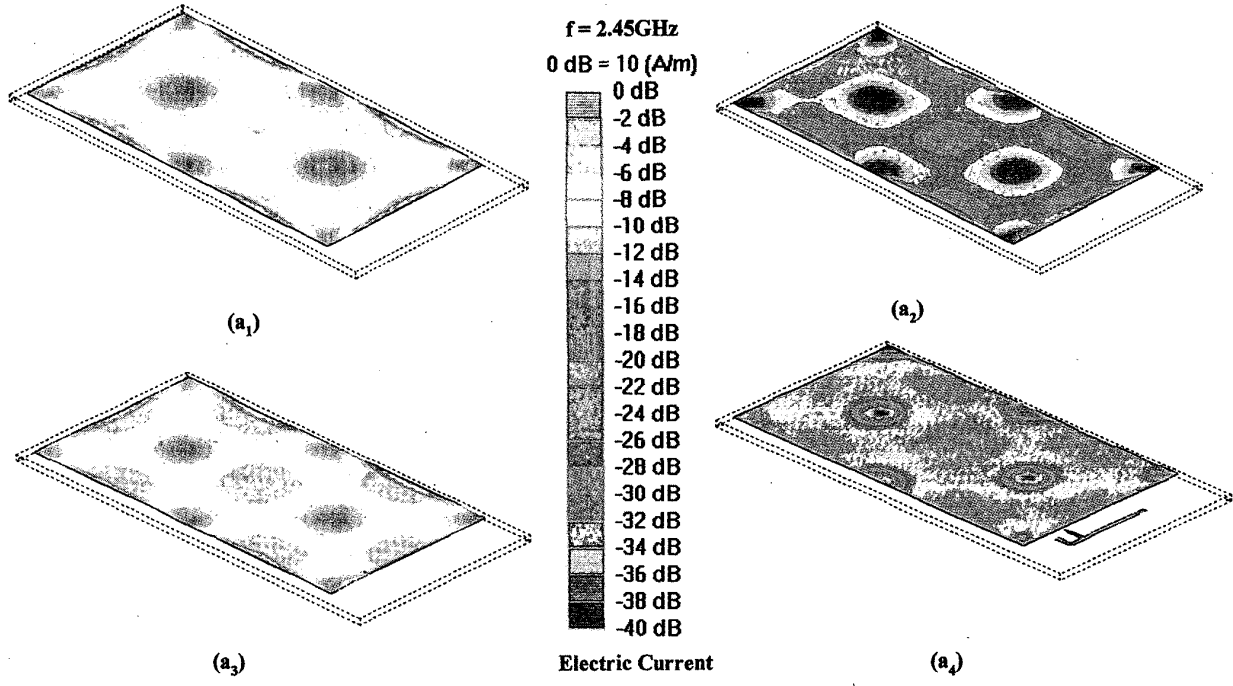


Figure 5a. The average current densities on the four layers of the PCMCIA card when the layers are unconnected.

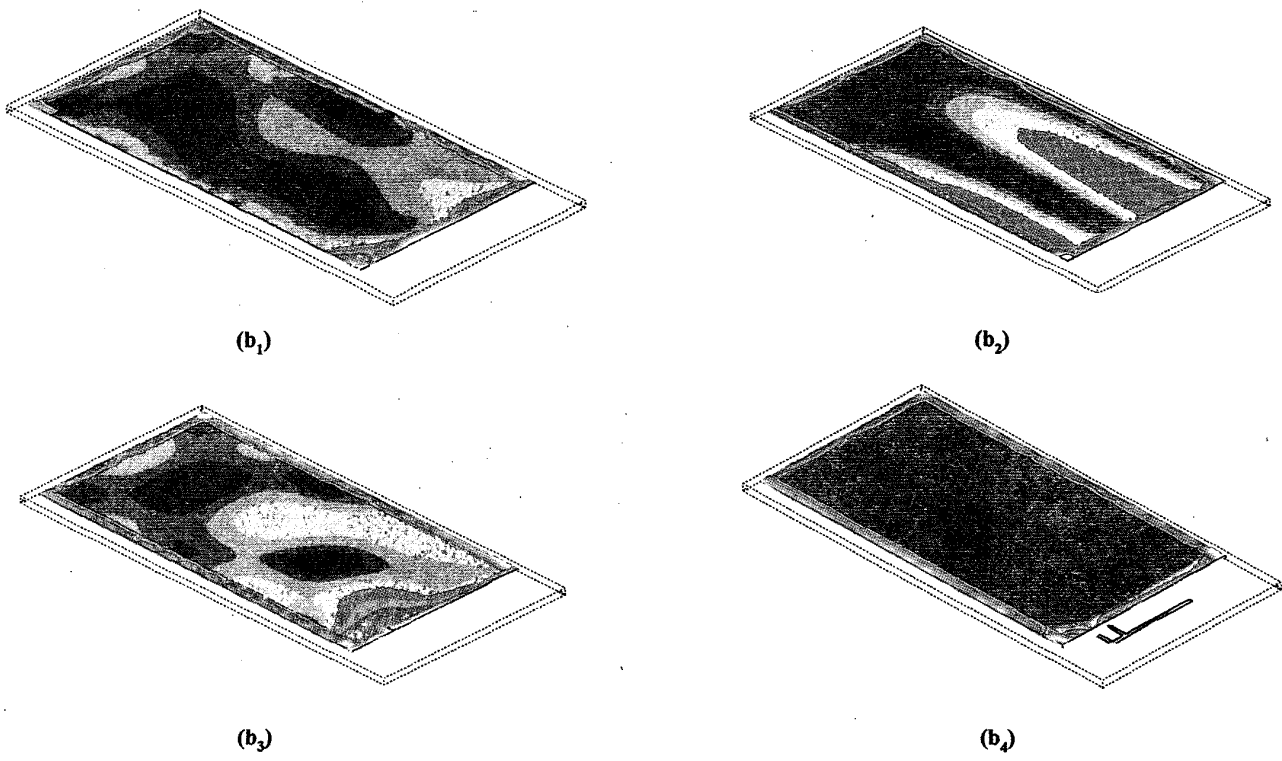


Figure 5b. The average current densities on the four layers of the PCMCIA card when the layers are connected.

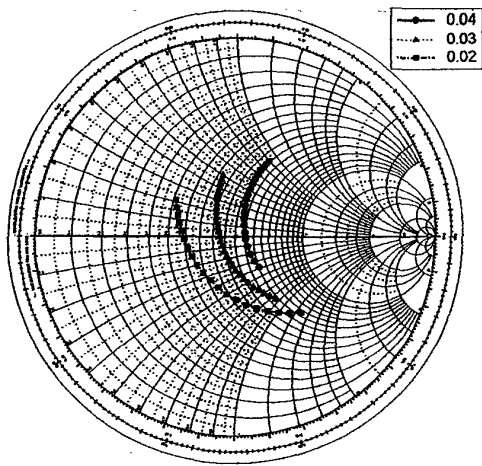


Figure 7a. The input impedance of the printed IFA as a function of the normalized length, h .

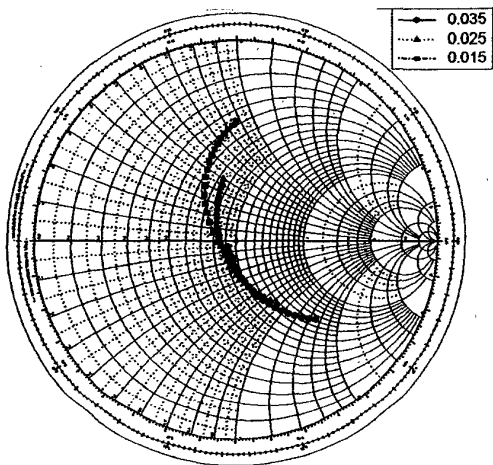


Figure 7b. The input impedance of the printed IFA as a function of the normalized length, d .

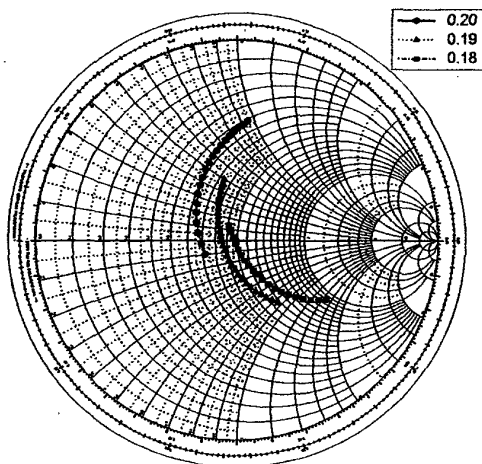


Figure 7c. The input impedance of the printed IFA as a function of the normalized length, l .

Table 2. The effect of the controlling parameters h , d , and l on the resonant frequency.

h/λ_0	l/λ_0	d/λ_0	f_{res} (GHz)
0.02	0.19	0.025	2.48
0.04	0.19	0.025	2.38
0.03	0.18	0.025	2.55
0.03	0.20	0.025	2.30
0.03	0.19	0.015	2.31
0.03	0.19	0.035	2.60

Table 3. The length of the IFA relative to a free-space quarter wavelength.

Frequency (GHz)	2.4	2.4415	2.484
$\lambda_0/4$ (mm)	31.25	30.7	30.2
Length Reduction (%)	10	8.5	7

Table 4. The electrical characterization of antennas [12, 13].

Thickness Class	L/r_0	r_0/λ_0
Very thin	5000	$r_0/\lambda_0 < 10^{-3}$
Thin	50	$10^{-3} < r_0/\lambda_0 < 5 \times 10^{-3}$
Thick	10	$5 \times 10^{-3} < r_0/\lambda_0 < 25 \times 10^{-3}$

parameters of the antenna affect both its input resistance and reactance. As the height, h , increased, the input resistance also increased, and the antenna became more inductive, since the horizontal part of the antenna moved away from the ground plane. By increasing the distance between the legs, d , the input resistance increased, and the antenna became capacitive. As far as the horizontal length is concerned, by increasing its value, the input resistance decreased, and the antenna became inductive.

Furthermore, Table 2 illustrates how alterations of the above three parameters affect the resonant frequency of the antenna. As h and l increased, the resonant frequency decreased, and vice versa. This was expected, since the height, h , and the length, l , affect the total length, L , of the IFA. On the other hand, as d increased, the resonant frequency increased, and vice versa.

From the above analysis, it is apparent that a combined change of the three parameters is necessary in order to fine-tune the antenna. This gives freedom to the antenna designer to modify the dimensions of the IFA, according to the available antenna space on the card or to the restrictions he or she might have. For instance, assuming that the horizontal part needs to be shorter, the distance d must also be shortened, in order to achieve a resonance at 2.45 GHz. As a conclusion, the three controlling parameters provide sufficient flexibility regarding the matching of the antenna. As has already been mentioned, the physical length of the implemented IFA was $L = 28.1$ mm, which, compared to the free-space quarter wavelength, $\lambda_0/4$, was reduced by the percentages shown in Table 3. Thus, the optimum IFA's length, in order to be fine-tuned, was found to be 8.5% shorter than $\lambda_0/4$ at the middle frequency of the band.

The flat metallic ribbon, which forms the printed IFA, can be thought of as a cylindrical wire with equivalent radius r_0 , given by the equation [12]

$$r_0 = 0.35t + 0.25w = 266.8 \mu\text{m}.$$

The IFA analyzed in this paper has $L/r_0 = 105$ and $r_0/\lambda_0 = 2.17 \times 10^{-3}$. Thus, according to Table 4, the IFA is thin. It is known [13] that the antenna bandwidth increases with its thickness. The antenna analyzed in this paper already has a bandwidth of 250 MHz, as shown in Figure 2, or 10.2% of the middle frequency for $VSWR \leq 2:1$. Consequently, the printed IFA can be tuned to operate in the 2.4 GHz ISM band with an even broader bandwidth if it is made thicker, by varying its cross-sectional dimensions according to Table 4. Other ways to enhance the IFA's bandwidth are an increase of the height, h , and the use of parasitic elements [11]. Thus, the printed IFA is an appropriate antenna to support not only the current generation of wireless-communication systems – which require a 1 MHz bandwidth for each of the 75 hopping frequencies – but also for the forthcoming generations, which the FCC is considering to have operate with 3 MHz and 5 MHz bandwidth for each hopping frequency.

5. Conclusion

In this paper, the analysis of an inverted-F antenna, printed on a PCMCIA card, was presented. This design is compact, efficient, easy and cost-effective to manufacture, and has an omni-directional pattern, mixed polarization, and a 250 MHz impedance bandwidth. Design guidelines for implementing a printed IFA – not only for current-generation short-range wireless-communication devices, but also for future-generation, wider-bandwidth devices – operating in the 2.4 GHz ISM band were additionally provided. The IFA's main design advantage is flexibility, because it can be tuned to function equally well in many wireless applications, without requiring modification of the fundamental design philosophy.

6. Acknowledgements

The authors would like to thank Dr. Jian Zheng, of Zeland Software, Inc., for his valuable advice and support.

7. References

1. Z. N. Chen, K. Hirasawa, K. W. Leung, and K. M. Luk, "A New Inverted F Antenna with a Ring Dielectric Resonator," *IEEE Transactions on Vehicular Technology*, VT-48, July 1999, pp. 1029-1032.
2. Rangestar International, Ultima Series, "Antenna Technical Overview."
3. R. J. P. Douville and D. S. James, "Experimental Study of Symmetric Microstrip Bends and their Compensation," *IEEE Transactions On Microwave Theory and Techniques*, MTT-26, 3, March 1978, pp. 175-181.
4. K. C. Gupta, R. Garg, I. Bahl, and P. Bhartia, *Microstrip Lines and Slotlines*, Second Edition, Norwood, MA, Artech House, 1996.
5. *IE3D Manual*, Zeland Software Inc.

6. *ADS Momentum Manual*, Agilent Technologies.

7. D. G. Swanson, Jr., "RF and Wireless Component Design Using Electromagnetic Simulation," CEI-Europe International Course, Davos, Switzerland, March 2000.

8. W. L. Stutzman, *Polarization in Electromagnetic Systems*, Norwood, MA, Artech House, Inc., 1993.

9. D. Chizhik, J. Ling, and R. A. Valenzuela, "The Effect of Electric Field Polarization on Indoor Propagation," IEEE ICUPC, Florence Italy, 1998.

10. M. Ali and G. Hayes, "Analysis of Integrated Inverted F Antennas for Bluetooth Applications," 2000 IEEE AP-S Conference on Antennas and Propagation for Wireless Communication, Massachusetts, November 2000, pp. 21-24.

11. K. Fujimoto, A. Henderson, K. Hirasawa, and J. R. James, *Small Antennas*, England, Research Studies Press Ltd., 1987.

12. C. A. Balanis, *Antenna Theory, Analysis and Design*, Second Edition, New York, John Wiley and Sons Inc., 1997.

13. W. L. Stutzman and G. A. Thiele, *Antenna Theory and Design*, Second Edition, New York, John Wiley and Sons Inc., 1998.

Introducing the Feature Article Authors

Constantinos Soras was born in Patras, Greece. He received both his electrical engineering diploma and PhD from the University of Patras, Greece, in 1981 and 1989, respectively. From 1982 to 1989, he was a Research Associate in the Electrical and Computer Engineering Department of the University of Patras, involved with modeling the performance of photovoltaic systems. Since 1991, he has served as a Lecturer in the Laboratory of Electromagnetics of the same department. He teaches the basic electromagnetic courses, and senior undergraduate/graduate-level computational electromagnetics. His current research interests focus on computational electromagnetics, printed antennas, indoor radio-wave propagation, and photovoltaic systems. He is a member of the IEEE, the Applied Computational Electromagnetics Society, the International Solar Energy Society, and the Technical Chamber of Greece.

Manos Karaboikis was born in Athens, Greece, on November 11, 1974. He received his electrical engineering diploma from the University of Patras, Greece, in 1999. Currently, he is a postgraduate student in the Laboratory of Electromagnetics, Department of Electrical and Computer Engineering of the University of Patras. His research interests include numerical solutions to electromagnetic radiation and scattering problems, printed antennas, and diversity antenna systems. He is a member of the Technical Chamber of Greece.

George Tsachtsiris was born in Kalamata, Greece, on September 16, 1976. He received his electrical engineering diploma from the University of Patras, Greece, in 1999. Currently, he is a postgraduate student in the Laboratory of Electromagnetics, Department of Electrical and Computer Engineering of the University of Patras. In May, 2000, he received the "Award of Excellence in Telecommunications" from Ericsson for his thesis. His research

interests include numerical solutions to electromagnetic radiation and scattering problems, printed antennas, and antennas of fractal geometry. He is a member of the Technical Chamber of Greece.

Vassilios Makios was born in Kavala, Greece. He received his electrical engineering degree (Dipl.Ing.) from the Technical University in Munich, Germany, in 1962, and the PhD (Dr.Ing.) from the Max Planck Institute for Plasma Physics and the Technical University in Munich in 1966. From 1962-67, he was a Research Associate in the Max Planck Institute for Plasma Physics in Munich, where he was associated with microwave interaction studies on plasmas. He served as Assistant Professor, 1967-70, Associate Professor, 1970-73, and full Professor, 1973-77, in the Department of Electronics, Carleton University, in Ottawa, Canada. There, he was involved with teaching and research in microwave and optical communications, radar technology, remote sensing, and CO₂ laser development. Since 1977, he has been an Honorary Research Professor of Carleton University. Since 1976, he has been a Professor of Engineering and Director of the Electromagnetics Laboratory in the Electrical Engineering Department of the University of Patras in Greece. He is involved in teaching and research in microwave and optical communications, data-

communications networks, LANs, MANs, B-ISDN, and ATM technology, with emphasis on efficient hardware implementations and rapid prototyping. He is also involved in research in photovoltaic systems. His laboratory is actively participating in EU ACTS and ESPRIT R&D projects, e.g., LION, DISTIMA, PANORAMA, COBUCO, etc. He spent his sabbatical years in 1986-1987 at the R&D laboratories of Siemens, in Munich, and in 2000-2001 at the University of California, Berkeley, and at GMD Fokus, in Berlin. He has published over 130 papers and numerous patents in the above fields. He has participated in the organizing committees of numerous IEEE and European conferences. He was the Technical Program Chair of the 5th Photovoltaic European Community Conference in Athens, 1983, and Co-Chair of the EURINFO 1988 Conference of the European Community. He is the recipient of the Silver Medal (1984) and the Gold Medal (1999) of the German Electrical Engineering Society (VDE). He is a Senior Member of the IEEE, a member of the Canadian Association of Physicists, the German Physical Society, and the VDE, a Professional Engineer of the Province of Ontario and the Greek Technical Chamber. He served as Dean of Engineering in the periods 1980-1982 and 1997-1999. For the past twelve years, he has served as the Vice President of the Research Committee of the University.



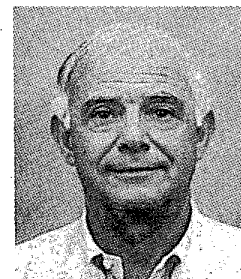
Constantinos Soras



Manos Karaboikis



George Tsachtsiris



Vassilios Makios

Editor's Comments *Continued from page 36*

the terminology and standards associated with this field are new to many who do not come from a communications-engineering background. Furthermore, the status of development of the standards, and of products and technology to implement them, can also be confusing. In the Wireless Corner, edited by Tuli Herscovici and Christos Christodoulou, Ramiro Jordan and Chaouki Abdallah provide a very nice overview of this field. Their introduction to the terminology and standards is easy to understand, and should be of considerable value to anyone working in this field. They also provide a very good summary of the developments to date in wireless LANs, as well as giving insight into the challenges remaining, and the likely near-term directions the technology will take.

Tuli and Christos are looking for contributions to the Wireless Corner. Again, here is a great opportunity!

Congratulations!

Allan Schell, overall Chair of the Awards and Fellow Committee, reports on the latest recognition given to AP-S members in this issue. Bob Hansen, one of the founders of AP-S, has been selected to receive the IEEE's 2002 Electromagnetics Award. Raj Mittra was selected to receive the 2002 AP-S Distinguished

Achievement Award. As we were going to press, it was announced that Don Dudley has been selected to receive the 2002 Chen-To Tai Distinguished Educator Award (information on this will be in Allan's report in the April issue).

Also listed in the report in this issue are the AP-S members who have been elected Fellows of the IEEE for 2002. Our sincere congratulations to all of them for receiving this very high honor – but a special word of recognition to Allen Glisson. Allen has been a part of the *Magazine* Staff for more than 18 years, and his contributions – in all areas – are greatly appreciated.

New Copyright Forms

The IEEE has just adopted a new "Copyright Transfer and Export Control Compliance Form," and new procedures associated with it. From now on, a signed original copy of this form must be received with any paper submitted for review or publication by the IEEE. More explicitly, this now means that the form has to be received *before* the review of an article for the *Magazine* or of a paper for the *Transactions* or the *Antennas and Wireless Propagation Letters (AWPL)* can be initiated. Failure to include the form will result in a delay in the start of the review process until a signed form is received.

Continued on page 54